Energy & Buildings 328 (2025) 115185

Contents lists available at ScienceDirect

Energy & Buildings

journal homepage: www.elsevier.com/locate/enb

Non-renewable energy demand reduction and positive energy buildings in Southern Europe's urban forms

Luigi Schibuola, Chiara Tambani *

University IUAV of Venice, Dorsoduro 2206, Venice 30123, Italy

ARTICLE INFO

Keywords:
Greenhouse gas emission (GHG)
Zero emission building (ZEB)
Local climate zone (LCZ)
Building dynamic simulation
Heat pump
PV system
Positive energy building (PEB)

ABSTRACT

The challenge of achieving a significant reduction in greenhouse gas emissions within a short timeframe necessitates extensive renovations of the existing building stock to meet the target of zero-emission buildings (ZEB). This study explores the feasibility of such renovations through building-plant system simulations for typical urban forms found in Southern Europe, classified using the Local Climate Zones (LCZ) method. Envelope retrofitting, combined with the use of electric heat pumps, allows for substantial reductions in energy demand while eliminating the use of fossil fuels. Renewable energy generated by rooftop photovoltaic systems can cover up to 96% of electric demand in the best case scenarios. However, results indicate that fully eliminating the need for electricity imports from the grid is unfeasible. Consequently, the more attainable goal of achieving a Positive Energy Building (PEB) status is investigated. In this context, a new definition of PEB is introduced, balancing the exported PV energy exclusively against the non-renewable portion of imported energy. Even when this PEB condition is met on an annual basis, it is not consistently sustained on a monthly level. The study concludes that achieving a monthly PEB target requires not only building-specific interventions but also an increased share of renewable energy supplied by the grid.

1. Introduction

1.1. Background and context

A significant portion of greenhouse gas (GHG) emissions, the primary driver of climate change, arises from the high energy consumption of the building sector [1,2]. Specifically, in European Union countries, this share accounts for approximately 40 % of total energy demand [3]. In response, the European Parliament has implemented various directives aimed at improving energy efficiency in buildings [4,5]. These regulations encompass energy certification requirements and the establishment of minimum energy performance standards. The 2010 recast of the Energy Performance of Buildings Directive (EPBD) [6] introduced the concept of nearly Zero Energy Buildings (NZEBs), defined as buildings with very high energy performance, where the low or nearly zero energy demand should be covered predominantly by energy from renewable sources, including energy produced on-site or nearby. Member states were tasked with establishing technical specifications for NZEB standards, which became mandatory for new private buildings after 2020, and for public buildings from 2018 onwards.

The most recent EPBD recast, published in May 2024 [7], advances beyond the NZEB concept, placing a stronger emphasis on reducing GHG emissions associated with fossil fuel-based energy production. The ultimate goal is the decarbonization of the European building stock by 2050. This target is to be achieved incrementally, with a 55 % reduction in GHG emissions by 2030 compared to 1990 levels [8]. Given that approximately 75 % of existing buildings in the EU do not meet current energy standards [7], it is clear that the EPBD's scope must extend beyond new construction to include the renovation of existing buildings. Member states must transpose the directive into national legislation by May 2026 and develop plans to ensure that both public and private buildings, residential and non-residential, are renovated to achieve zero-emission standards [9].

To attain zero-emission buildings, the first step involves reducing energy demand. Typical measures include building retrofits, installing

Abbreviations: ASHP, air source heat pump; DHW, domestic hot water; EPBD, Energy Performance of Buildings Directive; ESEER, European Seasonal Energy Efficiency Ratio; EXP, PV energy exported; GHG, greenhouse gas emission; GWHP, ground water heat pump; HP, heat pump; HVAC, heating ventilation and air conditioning systems; LCZ, local climatic zone; NRDEL, non-renewable quota of the electric energy delivered from the grid; NZEB, near zero energy building; PEB, positive energy building; PVSPB, photovoltaic simple payback; WUDAPT, World Urban Database and Access Portal Tools; ZEB, zero emission building.

* Corresponding author.
E-mail address: chiara.tambani@iuav.it (C. Tambani).

https://doi.org/10.1016/j.enbuild.2024.115185
Received 4 October 2024; Received in revised form 26 November 2024; Accepted 10 December 2024
Available online 15 December 2024

Nomenclature

NC	normalized capacity P_{fl}/P_{nom} (-)
NR	capacity ratio P/P_{fl} (−)
COP	coefficient of performance in heating mode (−)
EER	energy efficiency ratio in cooling mode (−)
P	actual capacity of the heat pump (kW)
P_{fl}	full load heat pump capacity (kW)
P_{nom}	nominal heat pump capacity (kW)
PLF	part load factor (−)
%PV	percentage quota of produced PV energy used by the building
%F	percentage quota of the building demand covered by PV energy
%PEB	percentage PEB index

photovoltaic (PV) systems on rooftops, and integrating electric heat pumps (HPs), which reduce a building's demand to mostly electrical energy, offsettable by self-produced PV electricity [10,11]. Thus, this option was always considered in this study. The introduction of electric HPs can reduce a building's energy demand to only electrical energy, which can be partially offset by self-produced PV electricity [12–15]. Consequently, buildings become "prosumers," i.e., producers and consumers, with their performance determined by the balance between energy production and consumption. In this context, a building's classification can be based on the concept of a Positive Energy Building (PEB), which refers to a building that generates more energy than it consumes.

1.2. Positive energy buildings (PEBs) and their role

PEBs represent an evolution in sustainable architecture, focusing not only on energy self-sufficiency but also on active contributions to energy systems. Unlike traditional approaches where energy-efficient buildings simply aim to minimize consumption, PEBs encompass a broader scope, often producing more energy than they use. This concept stems from the evolution of NZEBs and has gained significant attention in both research and European Union policy development [16–21].

PEB definitions in the literature vary, but generally emphasize an energy balance where renewable energy production exceeds consumption, often within a defined timeframe and physical boundary. These definitions often categorize PEBs based on factors such as the type of energy generated, its use for heating, cooling, ventilation, lighting, and other demands, as well as the dynamics of energy export and import [22,23].

Key interpretations include:

- A PEB produces more energy on-site than it consumes, covering all primary energy demands of the building [24]
- The net-positive balance signifies that the energy exported to the grid surpasses energy imported [25].
- PEBs may involve exporting surplus energy to other buildings or the grid, thus supporting local energy systems [18].
- An energy-efficient building with high self-consumption and flexibility can be considered a PEB [26].

The general criterion for a PEB is that it produces more energy than it consumes, feeding renewable energy to the grid.

However, a more accurate and precise approach, aimed at environmental decarbonization, must focus on eliminating the non-renewable energy share required by the building. A building's carbon footprint can be classified by assessing its contribution to GHG emissions, which stem from the use of non-renewable energy. Various PEB definitions exist in the literature, most do not distinguish between renewable and non-renewable energy in the energy balance. For most buildings, the electricity produced onsite comes from PV systems, making it renewable energy. On the other hand, grid electricity is composed of both non-renewable sources (e.g., thermal or nuclear power plants) and renewable sources (e.g., solar, wind, geothermal, biomass, and hydropower). In this perspective, the PEB should not merely balance energy flows but aim to eliminate non-renewable energy dependency. A novel definition thus emerges: a PEB is one where renewable energy exported exceeds any non-renewable energy imported, thereby minimizing carbon footprint.

The chosen metric for weighting and comparing energy carriers in building energy demand and production is pivotal in assessing PEBs. All energy balance items should be converted using the same metric. The two most relevant metrics are final energy and primary energy [23]:

- Final Energy is directly measurable and more transparent for end-users, providing a straightforward view of energy used without accounting for conversion losses.
- Primary Energy accounts for upstream impacts of energy carriers, making it essential for decarbonization-focused policies. The EPBD promotes primary energy metrics, as they better reflect environmental impacts [27–29].

For this study, primary energy was used as the metric.

The timeframe for assessing a building's energy balance can significantly influence PEB qualification. Annual balances are common for both NZEB and PEB criteria, aligning with regulatory norms [30–33]. However, adopting monthly balances may more accurately reflect energy production-consumption dynamics, particularly in climates with significant seasonal variation. A monthly analysis approach, alongside the annual balance, can also capture the variability in renewable energy generation and demand throughout the year [19]. For this reason, this study incorporates both annual and monthly balances. In both cases, the results are derived from an hourly assessment of the balance between renewable energy exported to the grid and the non-renewable energy supplied by the grid.

1.3. Influencing factors: Retrofitting, building types, electrified heating and climate

Attaining PEB status requires a substantial reduction in energy demand, which can be achieved through several strategies [34].

1. Demand Reduction in Heating and Cooling: Reducing energy demand through building envelope improvements, such as enhanced insulation, is a primary step in minimizing heating and cooling needs. This is especially crucial for buildings in colder climates, where heating demand is higher [35,36].
2. Energy-Efficient Equipment and Low-Energy Technologies: The installation of high-performance appliances and systems is essential for energy conservation. Advances in low-energy systems can significantly reduce operational energy needs.
3. Integration of Renewable Technologies and Electrified Systems: Incorporating renewable energy sources, such as PV systems, is central to PEBs [37]. Electrified systems, particularly those based on heat pumps, offer efficient heating and cooling while minimizing environmental impacts [38–41].

To generalize the outcomes, this study employed typical retrofit interventions based on all three listed strategies.

A building's energy demand is, also, strongly influenced by its form and the characteristics of the surrounding urban area [23,24]. Structural features, geometry, and opportunities for integrating energy systems vary significantly and are critical factors in determining the feasibility of achieving PEB status To generalize these complexities, urban areas can be systematically classified using the Local Climate Zones (LCZ) framework [25]. LCZs offer a standardized classification system to describe the physical and thermal properties of both urban and rural environments. For this reason, in this study, starting from an existing building, various building forms were identified through a comprehensive classification of the most common urban contexts using the LCZ methodology.

Also, climate significantly impacts PEB performance, influencing both heating/cooling demand and renewable generation capacity. Regional climate variations are a critical consideration in designing and retrofitting PEBs, affecting energy consumption and on-site renewable generation. In this study, the ASHRAE climate zone classification [42] was employed to generalize simulation findings, facilitating the extrapolation of results to other regions [43,44].

1.4. Study objectives

This study presents a novel approach using the LCZ methodology to classify buildings and evaluate their potential to achieve ZEB or PEB status. The analysis focused on retrofitted buildings, employing high-efficiency HPs and maximizing rooftop PV systems. The study was conducted using annual dynamic simulations on an hourly basis in EnergyPlus [45]. These simulations provided hourly values for heating, cooling, and other electric demands (e.g., appliances, lighting). EnergyPlus also modelled PV production, providing hourly values of PV output. Using these data, a quasi-steady-state calculation procedure based on a spreadsheet model was developed to calculate the hourly performance of the HP and, consequently, the total electric demand of the building, as well as the behaviour of the PV system, which was coupled with an electric storage model incorporated into this procedure. The study highlighted the importance of optimizing electric storage system sizes for each scenario, as fluctuations in energy demand and PV production significantly affect battery efficiency. The proposed new PEB approach was analysed on an annual balance basis and coupled with a monthly balance evaluation. In both cases, results were derived from the hourly balance between the renewable energy exported and the non-renewable energy supplied by the grid operator. A new %PEB index was proposed to quantify the effectiveness of the implemented solutions.

A key strength of this study lies in the detailed analyses tailored to Southern Europe's specific climatic, construction, and energy characteristics. By rigorously modelling these variables, the study provides an in-depth examination of building energy performance under conditions that are highly relevant to this region. Such specificity is invaluable in developing targeted strategies and best practices for improving energy performance in climates and infrastructures similar to those of Southern Europe. Future research could expand upon this study by examining diverse climate, regional construction practices, standard and energy infrastructure, thereby enhancing the applicability of these insights to a broader array of contexts.

2. Materials and methods

2.1. The building

In Treviso, a real building located in the city center has been considered as the base for the following analyses. In Fig. 1a, a picture of the building is shown. This is a typical structure that served as a reference for its dimensions, urban context, availability of surfaces for photovoltaic installation, and shading conditions. This building has 7 floors, with the ground floor used for commercial activities and the other 6 floors occupied by residential units. Specifically, there are 4 dwellings per floor. Each floor has an area of 345.5 m^2, and the total height of the building is 21 m. The original building lacks thermal insulation in the building envelope and is equipped with outdated heating systems. The objective of our study is to explore how to further reduce non-renewable energy dependence from the grid in a retrofitted building, where energy demand has already been minimized through typical retrofit actions. These initial retrofit actions included a thermal coat for the external walls, the addition of an insulation layer under the roof tiles, and the installation of more thermally efficient windows. Additionally, a smart artificial lighting system with illuminance level control through sensors is foreseen. In summer, solar screens for the windows will be in operation during air conditioning hours. Achieving a high level of thermal insulation is required by national regulations [46].

Therefore, after the retrofit, the maximum thermal transmittance coefficients (U-values) allowed for the climate zone of Treviso (zone E, 2378 HDD) are not exceeded. Table 1 provides a description of the layers (from inside to outside) of the main components of the building structures introduced into the building model, along with the final U-values. The building is currently equipped with an old heating system, consisting of a centralized thermal power station and radiators. The air

Table 1
Characteristics and simulation parameters of the building.

Heating set point temp. (°C)	20
Cooling set point temp. (°C)	26
Heating schedule (h)	7am-9pm[a] or 7am-7pm[b]
Cooling schedule (h)	11am-7am[a] or 9am-7pm[b]
Occupancy(Pers/m^2)	0.035[a] or 0.1 or[b]
Appliances gain (W/m^2)	3[a] or 6[b]
Appliances gain schedule	7am-10pm[a] or 8.30am-12.30pm[b] and 3.30 pm-7pm[b]
Air change rate (ACH)	0.5[a] or 1[b]
Walls – U-value	Plaster (1.5 cm), polyurethane (12 cm) brick (40 cm), plaster (2 cm) – U = 0.22 W/m^2K
Windows U-value	Double – pane clear glass – U = 1.3 W/m^2K – SHGC = 0.54 (–)
Roof U-value	Plaster (1.5 cm), concrete (20 cm), polyurethane (14 cm), tiles (2 cm) – U = 0.20 W/m2K

[a] referred to [a]dwellings, [b]commercial areas.

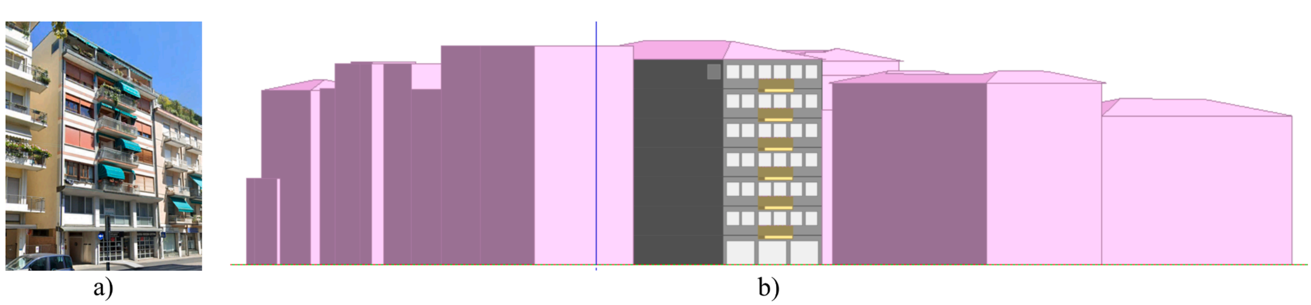

Fig. 1. A picture (a) of the building and its model simulated (b).

conditioning systems are limited to a small number of split units. However, in Italy, there is a growing trend towards the widespread use of air conditioning in buildings. For this reason, the application of a HP system was considered for both heating and air conditioning throughout the entire building, using fan-coils as terminal units. The hourly energy loads of the building were simulated using EnergyPlus, with the model developed in DesignBuilder [47], as shown in Fig. 1b. The main characteristics and simulation parameters of the building are provided in Table 1.

With reference to the LCZ classification of urban areas, the seven-story building analyzed in this study was selected to represent an area classified as LCZ 2 (compact midrise.). The fundamental parameters that define each LCZ include building height and spacing, percentage of permeable surfaces, tree density, and soil moisture [48]. Seventeen LCZ types have been introduced, ten of which are related to urban canopy characteristics, while the remaining seven are associated with land-cover types. Most methods used to determine the appropriate LCZ for an urban area rely on an automatic LCZ mapping procedure proposed by [49] which has been adopted by the World Urban Database and Access Portal Tools (WUDAPT) project to generate consistent LCZ maps for entire cities [50,51]. However, the majority of the urban center is characterized by three compact LCZ typologies: LCZ 1 (compact high-rise), LCZ 2 (compact midrise), and LCZ 3 (compact lowrise) [25]. These LCZs are the most common typology in the urban centers of many European cities [52,53]. Special attention was given to evaluating the impact of building height on their energy performance. To this end, the height of the representative building was adjusted to create models corresponding to the other two LCZ types, while all other parameters were held constant. Reducing the building height to 3 stories reclassified it as LCZ 3 (compact lowrise), whereas increasing it to 12 stories reclassified it as LCZ 1 (compact highrise). This analysis was extended to the cities of Rome and Palermo, which represent different ASHRAE climate zones in southern Europe: Treviso (4A – Mixed Humid), Rome (3A – Warm Humid), and Palermo (3B – Warm Dry [42]). The main scenarios investigated are summarized in Table 2. All simulated scenarios used the retrofitted building as the baseline. To enhance the precision of certain evaluations, simulations were conducted on buildings with heights ranging from 3 to 12 stories, always using the 7-story building as a baseline.

2.2. The HP model

In this study, Ground Water Source Heat Pumps (GWHPs) are investigated as an alternative to ASHPs, due to the stable and favourable thermal properties of groundwater throughout the year. Treviso, located in the resurgence zone of the Veneto region in northern Italy, serves as the reference site due to its groundwater availability, facilitating GWHP installation [54,55]. The performance of GWHPs was compared to that of ASHPs, and this comparison was extended to the cities of Rome and Palermo. For the comparison between the GWHP and the ASHP, two similar machines are considered. The aim is to evaluate only the benefits of using groundwater as an alternative to outside air as the cold source/sink for the heat pump, avoiding other technical differences that could influence the HP performance. Both heat pumps are centralized for each building and are designed to fully provide heating in winter, cooling in summer, and DHW production throughout the year. Each HP has a single refrigerant circuit using R410A, with two equal scroll compressors operating in tandem. Consequently, a two-stage on/off control modulates the capacity in two steps: 50 % and 100 % of the full capacity. Evaporators and condensers are stainless steel plate heat exchangers, except in the ASHP where one exchanger is an air coil. For HP modeling, the required parameters are the full capacity and the efficiency. The full capacity (P_{fl}) is the maximum thermal power supplied by the heat pump in heating or cooling mode. In heating mode, the efficiency is defined as the ratio between the heating power provided and the electrical power consumed, known as the coefficient of performance (COP). In cooling mode, this efficiency is the ratio between the cooling power provided and the electrical power consumed, referred to as the energy efficiency ratio (EER). These data, obtained through standard test methods [56], are typically provided by manufacturers as a function of the thermal levels of the external fluids exchanging heat at the condenser and evaporator. Specifically, in this study, the data for the ASHP come from [57] and those for the GWHP come from [58].

For the fan-coils selected as terminal units throughout the building, the supply water temperature from the heat pumps is set at 45 °C for heating and 7 °C for cooling. Once the temperature levels for heating and cooling are fixed, the performance of the heat pumps can be expressed as a function of the temperature of the external fluid exchanging heat with the evaporator in heating mode or with the condenser in cooling mode. This external fluid is the inlet well water for the GWHP and the outside air for the ASHP.

Fig. 2a and 2b show the full load curves of the coefficient of performance (COPfl) and energy efficiency ratio (EERfl) for ASHP and GWHP in heating and cooling modes, respectively. For the ASHP, outside air is moved by fans installed in the unit, while for the GWHP, inlet water is supplied by a submersible pump installed in a well. Therefore, the EER/COP of the ASHP already includes the electric power consumption of the fan, while for the GWHP, the pumping electric consumption is considered separately.

The corresponding normalized capacity (NC) is also reported in Fig. 2a and 2b for heating and cooling modes, respectively. NC represents the capacity normalized with respect to the nominal value, i.e., it is the ratio between the full capacity (P_{fl}) and the nominal capacity (P_{nom}), as shown in Eq. (1).

$$NC = P_{fl}/P_{nom} \quad (1)$$

In heating mode, P_{nom} refers to an outside air temperature of 7 °C with a relative humidity of 90 % for the ASHP, and to an evaporator inlet water temperature of 10 °C for the GWHP. In cooling mode, the nominal capacity refers to a temperature of 35 °C at the condenser inlet, for both the GWHP water and the outside air in the ASHP. The introduction of NC allows the data from Fig. 2 to be used in the HP model for different nominal capacities, required by buildings of varying sizes. In fact, the hourly thermal load of each building, calculated through EnergyPlus simulations, determines the peak load during the year that must be met by the HP. Consequently, technical specifications from manufacturers indicate the appropriate HP size, and thus its P_{nom}.

During regular HP operation, the control system adjusts the actual capacity to match the building's load, which often results in part-load

Table 2
The main scenarios investigated.

Scenario	City	ASHRAE climate zone	Number of floors	LCZ classification	Heat pump type
1	Treviso	4A (Mixed Humid)			GWHP
2	Rome	3A (Warm Humid)	7	LCZ 2 (Compact mid-rise)	ASHP
3	Palermo	3B (Warm Dry)			GWHP
4	Treviso	4A (Mixed Humid)			ASHP
5	Rome	3A (Warm Humid)	3	LCZ 3 (Compact low-rise)	GWHP
6	Palermo	3B (Warm Dry)			ASHP
7	Treviso	4A (Mixed Humid)			GWHP
8	Rome	3A (Warm Humid)	12	LCZ 1 (Compact high-rise)	ASHP
9	Palermo	3B (Warm Dry)			GWHP

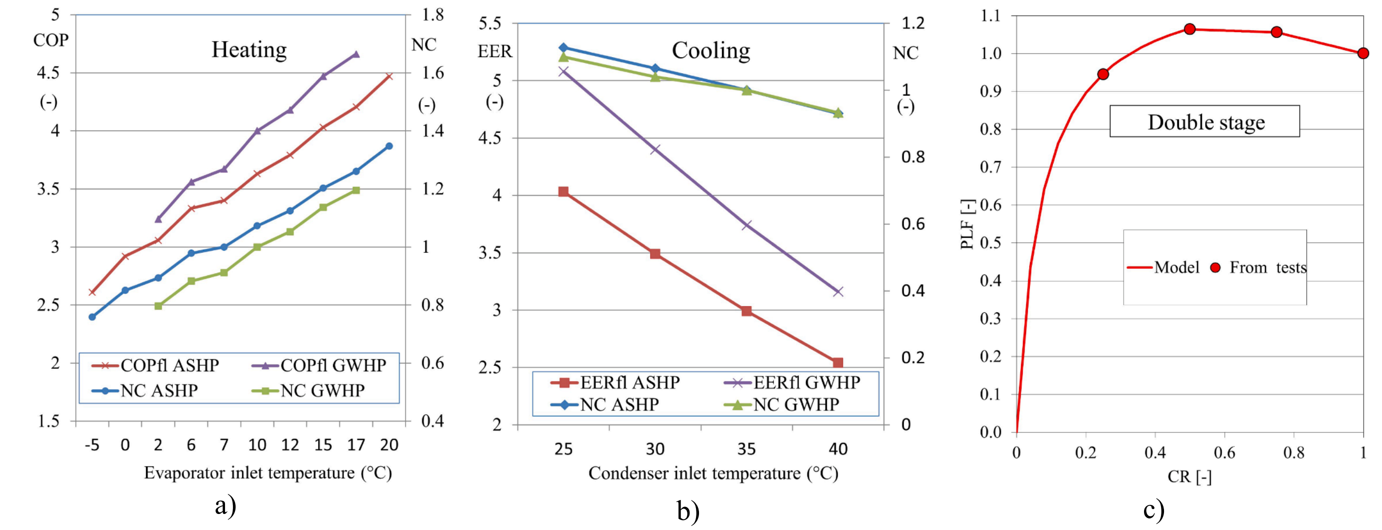

Fig. 2. COP_{fl} or EER_{fl} and normalized capacity NC as a function of temperature at evaporator inlet in the heating mode (a) or at condenser inlet in the cooling mode (b). PLF curve as a function of CR (c).

conditions that can affect performance. To account for the impact of part-load operation, a part-load factor (PLF) is calculated to correct the full-load efficiency, as deduced from Fig. 2a and 2b [59–61]. Fig. 2c illustrates the trend of the PLF as a function of the Capacity Ratio (CR), defined as the ratio between the actual capacity and the maximum capacity the HP can deliver under identical operating temperatures. Notably, since both GWHP and ASHP employ a similar multi-stage control system, this curve is applicable to both types of heat pumps.

It is noteworthy that the PLF exceeds one across a broad range of CR values, indicating that performance is enhanced under part-load conditions compared to full-load operation. This phenomenon arises because, with two compressors operating in the same refrigerant circuit, the evaporator and condenser are oversized when functioning at part-load compared to their performance at full load. The PLF trend is derived from part-load performance data at 25 %, 50 %, 75 %, and 100 % of the maximum capacity provided by the manufacturer. These data points, obtained from standard laboratory tests [62], were utilized by the manufacturer to calculate seasonal performance indices, including the European Seasonal Energy Efficiency Ratio (ESEER) [63]. Additionally, this data can be employed to determine the corresponding PLF [64] and to interpolate the PLF curves between the four measured points. For CR values below 25 %, the interpolation is replaced by a simplified algorithm recommended by EN 14825 for a single-stage on–off control [62].

For DHW production, the installation of a suitably sized DHW storage tank is considered for each building. During the time interval allocated for reloading this storage, the HP is entirely dedicated to this operation, generating hot water at 50 °C. Consequently, the COP specific to DHW production is calculated using the manufacturer's specifications.

The HP model employs a quasi-steady-state calculation procedure that utilizes a spreadsheet-style model applied to each building. At each hourly time step, the required HP capacity equals the building load *P*, as calculated by EnergyPlus. In heating mode, the COP_{fl} and the NC are represented in Fig. 2a as functions of the outdoor air temperature for ASHPs, or the inlet water temperature for GWHPs. From NC the P_{nom} permits to calculate the HP actual full capacity P_{fl} by Eq. (2) and consequently also the CR by Eq. (3).

$$P_{fl} = P_{nom} NC \tag{2}$$

$$CR = P/P_{fl} \tag{3}$$

Fig. 2c provides the PLF necessary to obtain the actual COP by eq. (4).

$$COP = COP_{fl}\, PLF \tag{4}$$

The electricity consumption of the HP is defined as the ratio of the actual capacity *P* to the simultaneous COP. The seasonal average COP is derived from the ratio of the heating energy supplied during winter to the corresponding electricity consumption over the same period. In cooling mode, the calculation procedure mirrors that of the heating mode, with the substitution of building cooling loads and HP performance data from Fig. 2b. For DHW production, the annual average COP is calculated as the ratio of the total annual DHW requirements met to the corresponding electricity consumption, employing a procedure akin to that used for building heating.

2.3. *The PV system*

To simulate PV production on the roof, we considered PV collectors characterized by high efficiency. Specifically, we referenced a type of panel equipped with mono-crystalline cells currently available on the market [65]. The principal characteristics of these panels are summarized in Table 3.

At an hourly time step, the performance of the PV system was simulated using the EnergyPlus PV model, which is based on the one-diode model [66,67]. In this model, the cell temperature is calculated using a dynamic approach developed by Ulleberg [68]. The equivalent one-diode model is a widely adopted method for simulating and analyzing the performance of PV modules. This model approximates the electrical characteristics of a PV cell by integrating an ideal diode, a current source representing the photocurrent generated by sunlight, a series resistance that accounts for internal resistive losses, and a parallel (shunt) resistance that captures leakage currents. The Ulleberg dynamic

Table 3
Principal data of the PV module.

Nominal Power	400 W
Nominal panel efficiency	22.6 %
Rated Voltage (Vmpp)	65.8 V
Rated Current (Impp)	6.08 A
Open-circuit Voltage (Voc)	75.6 V
Short-circuit Current (Isc)	6.58 A
Solar cells	104 Mono-crystalline
Module surface	1.046x1.690 = 1.758 m^2

simulation technique decouples electrical and thermal behaviors, allowing for a more accurate prediction of cell temperature. In this approach, the current cell temperature depends on the previous cell temperature and the thermal capacity of the PV module material. This method enables precise performance predictions of PV systems under varying irradiance and temperature conditions.

For each roof pitch, the PV production of an array was simulated using climatic data. While the number of installed modules can increase, particularly for larger pitches, their maximum number is ultimately constrained by the dimensions of the specific module type selected from the market. By reducing the size of individual modules, a greater roof area can be covered by the PV array. In other words, the total PV area that can be installed on a pitch depends on the model of the chosen module. To generalize the results regarding potential PV production, a theoretical limit condition was assumed, wherein the PV array covers the entire pitch area. This approach allows for the calculation of the maximum possible PV production for the considered roof. To determine the unitary PV production, the energy output of a simulated PV array was normalized by the surface area of the installed modules, providing a standardized production value per square meter. In detail, the simulation results for an array of 20 modules (35.16 m^2) were analyzed to derive the corresponding unit values for incident solar radiation and PV production per square meter for each pitch. The efficiency is defined as the ratio between PV production and solar radiation. The PV production for each pitch is calculated by multiplying the pitch area by the corresponding unitary PV production. Finally, the total PV production for the roof is obtained by summing the PV production across all pitches. These values are reported in Table 4 for each pitch and for the entire roof on an annual basis for the three considered localities. Notably, this PV production remains constant for all buildings with different numbers of floors simulated within the same city.

The possibility of incorporating electric storage through batteries was also considered. To simulate battery performance, a model was developed based on the characteristics of a typical lithium-ion battery pack available on the market [69]. In this case, a single pack can provide usable energy of 13.5 kWh, with a maximum charge or discharge power of 5 kW and a round-trip efficiency of 90 %. Instead of considering the installation of multiple packs, the model assumes the ability to continuously vary the total usable capacity of the storage. However, the ratio between the total effective maximum real power for charging or discharging and the total usable energy remains constant at 5/13.5≈0.37.

At each time step, the PV production not immediately consumed by the building charges the storage, with any surplus being exported to the grid. If PV production does not meet the building's demand, the battery discharges as much energy as possible, with the remaining demand supplied by the grid. The electric storage model operates on an hourly time step, balancing the electric energy initially present in storage with the electric flux of charge or discharge. This model calculates the new final electricity level accumulated, accounting for round-trip efficiency and the maximum power that can be exchanged.

For each building and locality, the size of the electric storage was optimized through a cost-benefit analysis. A cost of €480 per kWh was assumed for the batteries, reflecting the current price of the selected pack[70]. The primary benefit derives from the reduction in the amount of electricity purchased from the grid due to the presence of electric storage, compared to the same scenario without storage in the PV system. The corresponding economic benefit was calculated using a grid electricity cost of €0.26 per kWh, which is an average value for EU countries in 2024 [71].

Additionally, the exported PV production must be considered; this quota decreases as more PV energy is utilized on-site. Various methods and prices for selling exported electricity exist in Europe. In Italy, a dedicated withdrawal system is anticipated due to the elimination of on-site exchanges in the near future. Here, surplus PV energy is credited to the producer's account by GSE [72], the public energy services operator in Italy, with an assumed average purchase price of €0.10 per kWh [73]. Tax incentives for solar systems must also be factored into the annual benefit, as 50 % of their cost can be deducted over ten years. This tax reduction applies to the cost of electric batteries as well. In recent years, we have observed a significant reduction in the costs of energy storage systems, particularly lithium-ion batteries, whose prices have decreased by approximately 90 % from 2010 to 2023 [74]. However, the widespread adoption of electrical storage in photovoltaic systems still requires strong support policies. Many countries have introduced economic incentives, such as tax credits and subsidies for stored energy. These measures have proven essential for overcoming initial financial barriers, making storage systems accessible to a growing number of users and less dependent on upfront costs [75,76]. In this study, to size the electric storage, a payback period of 10 years was considered acceptable for the investment, which aligns with the typical warranty period offered by producers.

While discounted payback (DPB) analysis is generally the preferred method for such evaluations, the high variability of costs, prices, inflation, and discount rates anticipated over the next decade complicates these assumptions. Although DPB analysis may appear precise, it is often imprecise in practice. Therefore, a simple payback (SPB) analysis was deemed more realistic. The adoption of the simpler SPB method, which disregards the temporal penalty between the initial investment and subsequent returns, tends to yield a greater storage outcome compared to what can be achieved with the DPB method. Given the difficulty in accurately quantifying indices with the DPB method, the results from SPB therefore provide a precautionary margin. Moreover, this research is focused on investigating the building's maximum achievable performance, and thus the electric storage optimized through SPB can be considered the upper economic limit. As shown in the following Fig. 6, the storage optimized with SPB is also consistent with the stabilization of photovoltaic performance, which generally occurs beyond a certain storage capacity.

In this approach, the payback period is calculated as the ratio of the storage cost to the annual economic benefit. Consequently, the SPB method was used in this study to size the electric storage for each building across the three localities.

Table 4
Annual performances of the PV roof.

Roof pitch Orientation — Area	1 NW – 163.3 m^2			2 SE – 164.7 m^2			3 SW – 55.9 m^2			4 NE – 58.8 m^2		
	Treviso	Rome	Palermo	Treviso	Rome	Palermo	Treviso	Rome	Palermo	Treviso	Rome	Palermo
Incident radiation (kWh/m^2 year)	997.7	1166.1	1324.8	1166.2	1349.7	1546.4	1163.9	1347.2	1544.0	996.9	1165.2	1323.5
PV production (kWh/m^2 year)	167.1	209.1	266.6	222.4	272.4	345.9	221.4	271.2	344.9	167.0	209.1	266.2
Efficiency (%)	16.7	17.9	20.1	19.1	20.2	22.4	19.0	20.1	22.3	16.8	17.9	20.1
	Total PV production of the roof (kWh/m^2 year) (1 + 2 + 3 + 4)											
Treviso	86106.1											
Rome	106467.9											
Palermo	135438.9											

3. Results and discussion

3.1. Electrical demand of the buildings

The dynamic simulation of the buildings allows for the calculation of thermal loads and, consequently, the annual thermal energy requirements for heating, cooling, and DHW production. These results are illustrated in Fig. 3 for the three LCZ buildings across the three locations. Additionally, Fig. 3 reports the annual electrical demand for various uses, including lighting and appliances. As expected, for buildings of the same size, the heating requirement decreases while the cooling requirement increases from the North to the South of Italy. However, the DHW demand remains constant across the locations. The most significant climate-related variation is observed in the heating requirement, with considerably higher values recorded in Treviso.

Despite the fact that the electrical demand for various uses is not directly comparable to thermal requirements, it plays a significant role in the total energy balance of a building. For buildings of the same size, a slight variation can be observed across different cities, primarily due to the use of lighting sensors. Overall, this electrical demand aligns with expectations. Specifically, for a single dwelling unit, the average annual consumption is 1890 kWh/year, closely matching the value of 1912 kWh/year provided by statistical analyses for Italy [71].

In Fig. 4a, the annual COPs and EERs for all LCZ buildings in the three locations are reported. A notable improvement in efficiency is evident with the use of GWHP instead of ASHP, both for heating, cooling, and DHW production. The resulting annual electrical energy savings of the GWHP compared to the ASHP are expressed as percentages in Fig. 4b, for buildings with 3 to 12 floors in the three cities. Each city exhibits modest fluctuations in savings due to varying load profiles of the buildings. In Palermo, savings range from 15.8 % to 17.5 %, in Rome from 16.7 % to 18.8 %, and in Treviso from 21.8 % to 23.4 %. The highest energy savings are observed in Treviso, primarily due to the performance during winter. In fact, the higher heating demand in Treviso allows for maximizing the benefits of the GWHP, due to the combination of two positive effects: the improved temperature level at the evaporator inlet and the higher PLF. The use of GWHP leads to significant energy savings when compared to the annual electricity demand of heat pumps. However, due to the relatively high share of other electrical consumptions (such as lighting and appliances), the advantage of GWHP over ASHP has a limited impact on the overall distribution of the total electricity demand of the buildings.

This observation is clearly illustrated in Fig. 5, which displays the percentage distribution of the total electricity demand between the HP demand share and the share related to other electrical consumptions within the building. The data are presented for the three LCZ buildings and locations, comparing the use of ASHP and GWHP. The switch to GWHP from ASHP only slightly reduces the HP electricity demand as a proportion of the total electricity demand. Specifically, when considering the total electricity consumption of each building with an ASHP, the energy savings achieved by using a GWHP range between 3.7 % (Palermo, LCZ 1) and 8.4 % (Treviso, LCZ 3).

3.2. The influence of the electricity storage

The initial step involves optimizing the battery capacity, determined based on a financial analysis using the calculation of the SPB period, which must not exceed ten years. This optimization was performed for all buildings ranging from 3 to 12 floors across the three localities.

The results of the optimization process are presented in Fig. 6 for the case of the GWHP system. In Fig. 6, the percentage share (%PV) of the produced PV energy used in the building and the percentage fraction (%F) of the total building electricity demand covered by PV are plotted as functions of battery capacity for various building sizes in the three locations. The optimized battery capacities are highlighted with a larger red symbol for each building size.

In the case of no battery storage, Fig. 6 shows the %PV and %F values corresponding to the immediate use of PV energy in each building. The integration of electricity storage increases both %PV and %F, but these improvements tend to stabilize after reaching certain battery capacity thresholds, particularly in buildings with fewer floors.

In buildings with lower electricity demand, the %F is already high with minimal battery capacity. In such cases, further increases in capacity offer diminishing returns, as %F remains low during periods of modest PV production. As the building size and consequently electricity demand grow, the PV system struggles more to meet the demand, and increasing the battery capacity allows for a higher share of the demand to be met. However, this effect is again limited, as the remaining demand typically occurs during periods of low solar radiation. Thus, economic optimization places a cap on the benefits of increasing battery capacity.

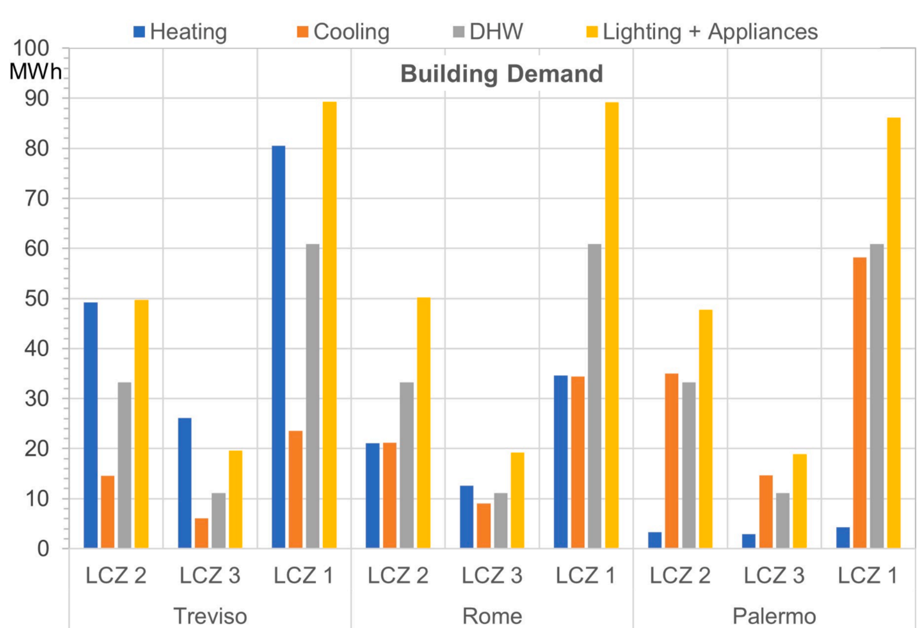

Fig. 3. Annual thermal requirements for heating, cooling, and domestic hot water (DHW) production for the three LCZ buildings in the three cities. The electric demand for lighting and appliances is also reported.

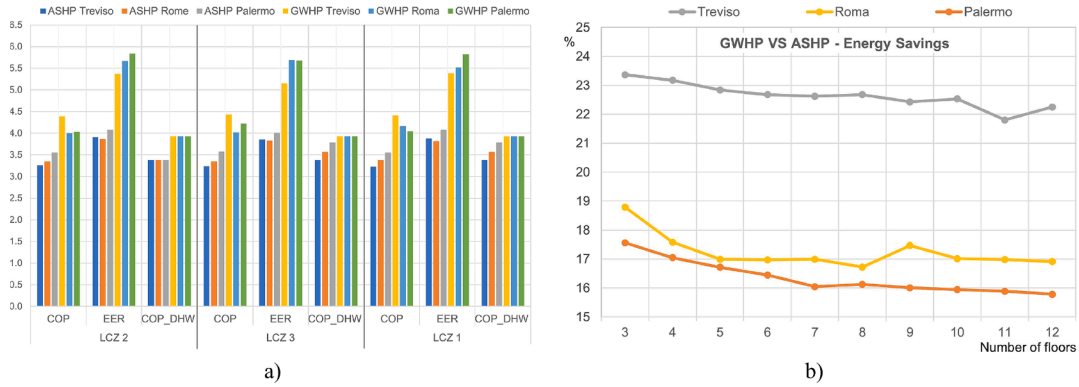

Fig. 4. Annual COP and EER for the LCZ buildings with ASHP and GWHP in the three studied cities a). Electric energy savings by GWHP compared to ASHP for buildings with different number of floors b).

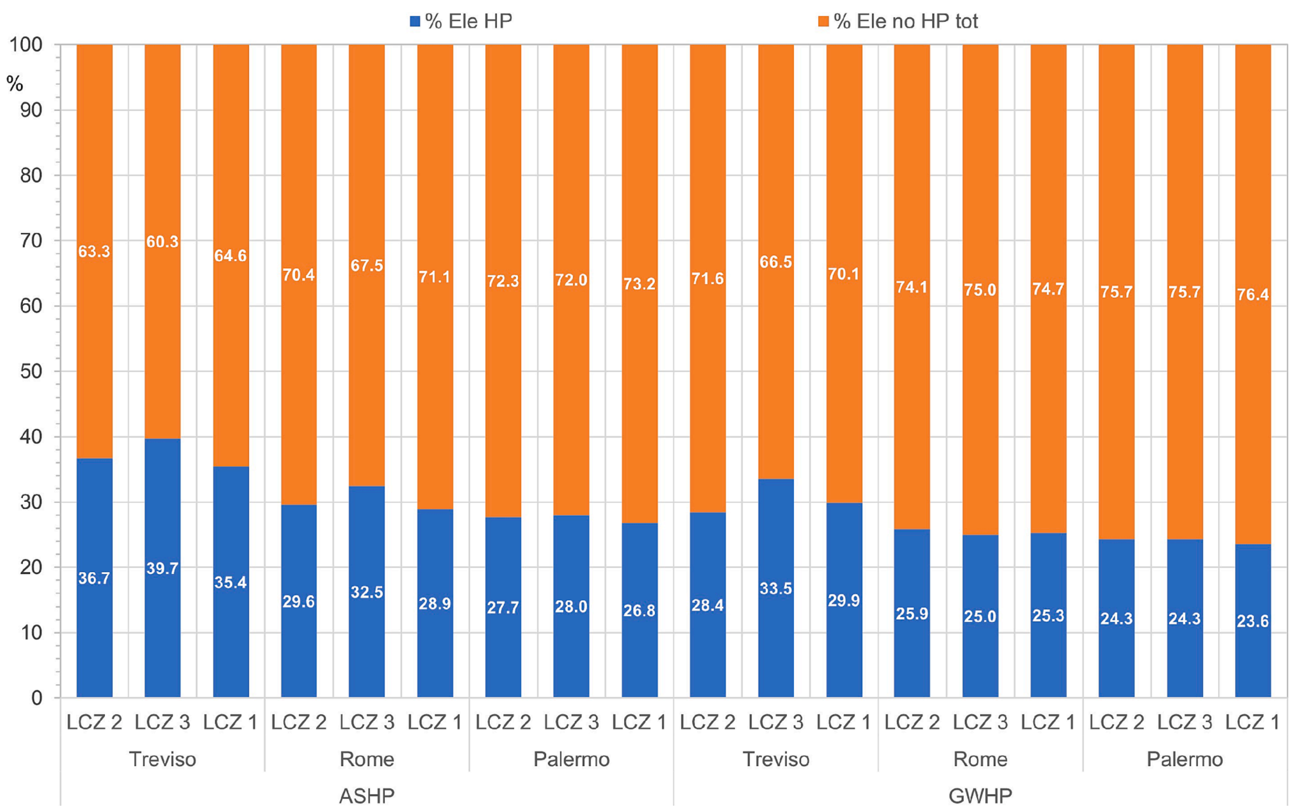

Fig. 5. Percentage distribution of the total annual electricity demand between the HP quota (%Ele HP) and the quota relative to the other consumptions (%Ele no HP) for the three LCZ buildings and locations with the presence of ASHP or GWHP.

In Treviso, the optimized battery capacity ranges from 40 kWh for a 3-floor building to 120 kWh for a 12-floor building. In Rome, the range extends from 55 kWh to 165 kWh, and in Palermo from 65 kWh to 210 kWh. As expected, the increase in PV production from Treviso to Palermo allows for better utilization of electric storage. However, the final optimized battery capacity is strongly determined by the building's electricity demand.

The optimization was also conducted for the case of ASHP systems. Due to the minimal variation in total electricity demand, the optimized battery capacities for buildings with ASHPs are the same as those for GWHPs.

3.3. *Calculation of the non-renewable energy provided by the grid*

Since the annual fraction of %F is always less than one, the analysis reveals that the PV system is unable to meet the total electricity demand in any of the buildings across the three localities. As a result, all buildings require a portion of their electricity to be supplied by the grid. Simultaneously, not all of the PV production is used on-site, and the surplus is exported to the grid. These findings are summarized in Fig. 7 for the two types of HPs (ASHP and GWHP).

Fig. 7 presents a comparison between %PV and %F obtained with ASHPs and GWHPs across the three LCZ buildings in different localities. The slight reduction in overall electricity demand due to the use of GWHP leads to a decrease in the local utilization of PV-generated energy, but it also increases the share of the building's total demand met by PV energy. Specifically, the percentage decrease in %PV ranges from 1.2 % (Treviso LCZ 1) to 4.8 % (Palermo LCZ 3), while the percentage increase in %F ranges from 0.3 % (Palermo LCZ 3) to 7.2 % (Treviso LCZ 1). Therefore, although GWHPs contribute to energy savings in the total

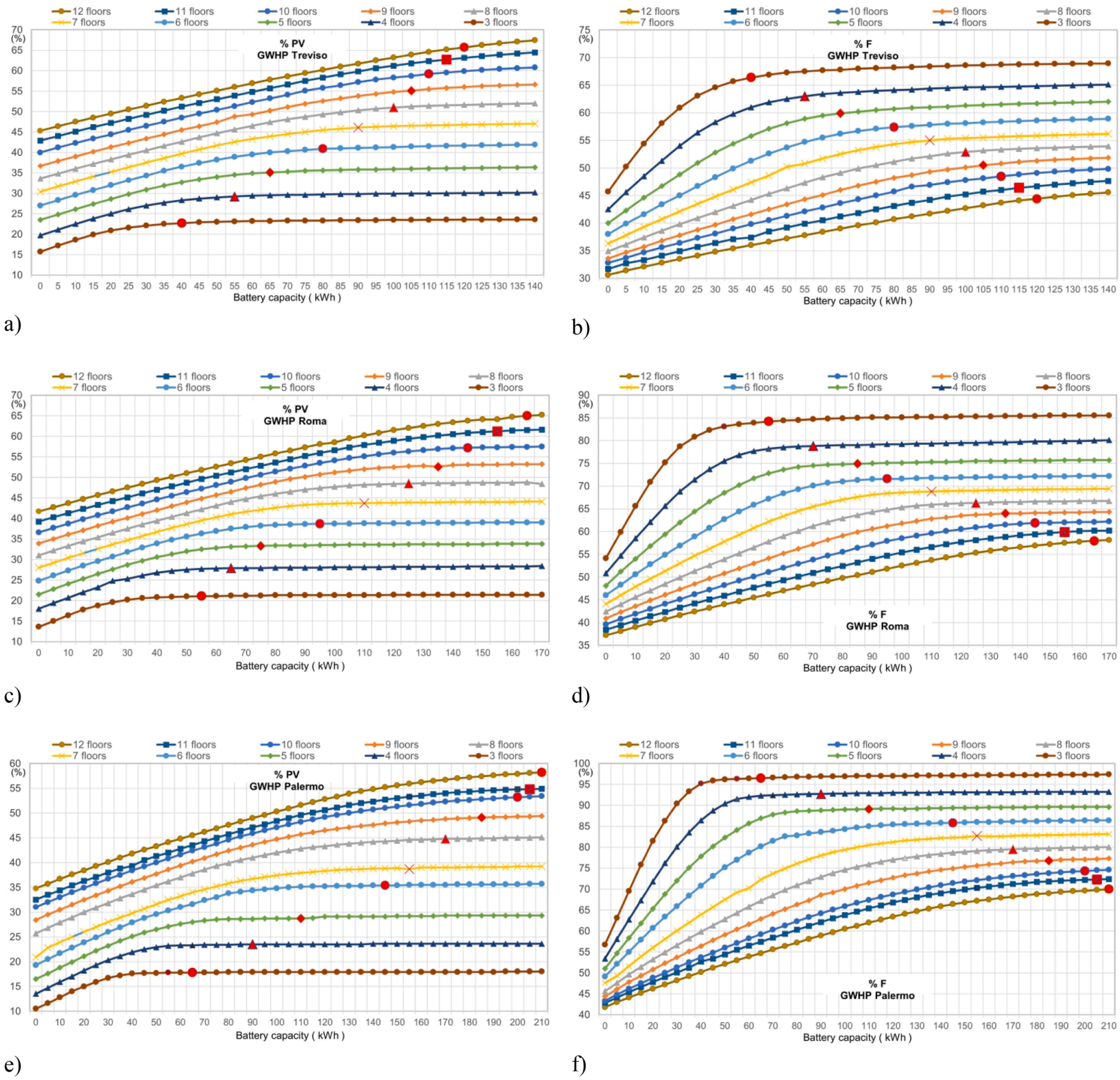

Fig. 6. %PV and %F as a function of battery capacity with GWHP for various building sizes in the three localities.

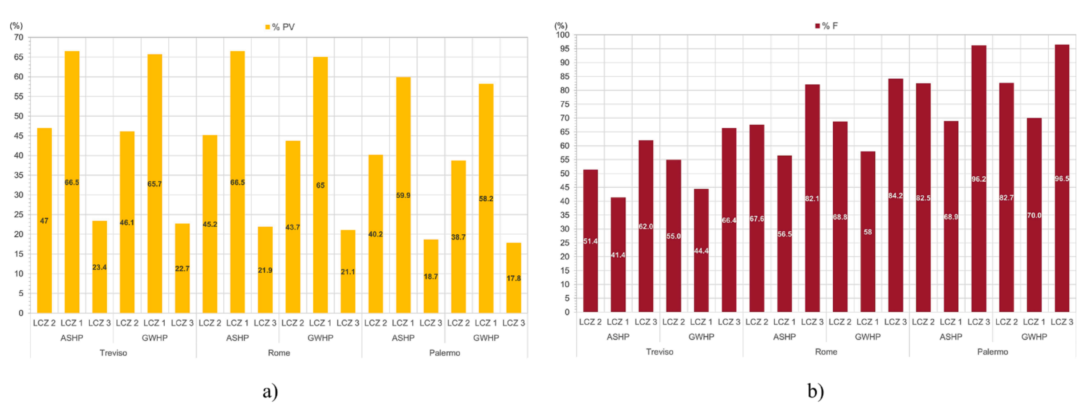

Fig. 7. %PV and %F b) for ASHPs and GWHPs in the three LCZ buildings and different localities.

electricity consumption of the buildings, they do not significantly enhance the on-site use of PV energy. Note that, in the best-case scenario, in Palermo with the LCZ 3 building, a %F exceeding 96 % is achieved with both heat pumps, although it does not reach 100 %. This occurs despite the significant availability of photovoltaic energy, with % PV ranging between 17.8 % and 18.7 %.

To generalize the results, following the EPBD directive, primary energy consumptions per unit surface area are calculated. For the conversion of electricity delivered by the public grid into primary energy, the official Italian conversion factor [77], set at 2.42, is used. This factor represents the sum of the conversion factors for the non-renewable portion (1.95) and the renewable portion (0.47) of energy produced by RES. Therefore, a final conversion factor of 1.95 is applied to calculate the non-renewable primary energy corresponding to the delivered electricity.

For buildings ranging from 3 to 12 floors, the annual non-renewable primary energy delivered by the grid, normalized by the building's unit area, is presented in Fig. 8a for both ASHP and GWHP solutions. Since the PV production remains constant across all buildings in a given city, the increasing total electric demand causes the specific delivered quota to rise. In these cases, the import of non-renewable energy cannot be reduced to zero, even for the smaller buildings, due to the limitations imposed by the available roof area for the PV system. The specific delivered energy ranges from 1.6 kWh/m2·yr (GWHP, 3-storey building in Palermo) to 38.3 kWh/m2·yr (ASHP, 12-storey building in Treviso). This analysis highlights the dependence of non-renewable energy consumption on building size and locality, despite the integration of PV systems. One possibility to improve the energy balance is to connect the buildings to a district heating network powered by renewable fuels, such as biomass or biogas. In this scenario, heating and domestic hot water (DHW) production are directly supplied by the heat from the network. During the summer months, the cooling energy required for air conditioning can be generated using local absorption chillers that utilize the heating network. This approach allows for the theoretical potential to achieve zero electrical consumption for heating, cooling, and DHW production.

In this case, a significant reduction in the electricity demand of the buildings can be realized. Fig. 8b illustrates the non-renewable primary energy delivered by the grid when excluding the demand for heating, cooling, and DHW production. As a result, the electricity storages are recalibrated based on this new, reduced electrical demand. This strategy not only enhances the overall energy efficiency of the buildings but also promotes the use of renewable energy sources, contributing to a more sustainable urban energy system.

With respect to Fig. 8a, the minimum value of non-renewable primary energy delivered by the grid decreases by 68.7 %, resulting in a new minimum of 0.5 kWh/m^2·yr for the 3-storey building in Palermo. Similarly, the maximum value is reduced by 51.2 %, now standing at 18.7 kWh/m^2·yr for the 12-storey building in Treviso.

When comparing these results to those in Fig. 8a, the reduction in non-renewable primary energy requirements is indeed significant. However, it is important to note that this strategy does not completely eliminate the need for non-renewable electricity from the grid. Despite the improvements, a portion of the electricity demand remains reliant on non-renewable sources, highlighting the ongoing challenge of achieving full energy independence in building operations.

3.4. The PEB verification

Another important aspect is the comparison between the renewable PV energy exported (EXP) from the building and the non-renewable quota (NRDEL) of the electric energy delivered from the grid. NRDEL was obtained through simulations that consider, on an hourly basis, the non-renewable energy supplied by the grid as the residual share, relative to the hourly renewable share provided by the grid. This data is provided by the grid operator, Terna, for the entire Italian network. The hourly renewable share profile used for the simulation corresponds to data from 2023 [78].

If the difference between EXP and NRDEL is greater than zero, the building can be defined as a PEB according to the new PEB definition proposed in this study. Naturally, this comparison can be done at different time scales: daily, monthly, or annually. To better represent this condition, a new index is introduced in this paper, named the percentage PEB index (%PEB). This index is defined as:

$$\%PEB = 100 \bullet \frac{EXP}{EXP + NRDEL} \quad (n).$$

Therefore, %PEB is the percentage ratio between EXP and the sum of EXP and the NRDEL quota. This %PEB can vary between 0 % and 100 %. If the exported and delivered quotas are equal, the %PEB is 50 %. Above 50 %, the building is a PEB, as the exported quota is greater than the non-renewable delivered quota. If %PEB is lower than 50 %, the building is not a PEB, as the exported quota is lower than the delivered one.

In Fig. 9a, the %PEB is reported on an annual basis for all building sizes in the three climatic conditions, starting from 0 %. The length of each histogram represents the numerical distance between each %PEB value and 50 %, which indicates the parity condition between imported and exported quotas. On an annual basis, all buildings up to 9 floors are PEBs. Beyond 9 floors, the increase in demand progressively reduces the number of PEBs, first in Treviso, and then also in Rome for 12-floor ASHP buildings. All buildings in Palermo are PEBs. Overall, the majority of the studied buildings appear to be PEBs on an annual basis, although this assessment changes significantly when we analyze electric energy exchanges with the grid on a monthly basis.

In Fig. 9b, 9c, and 9d, %PEB is reported on a monthly basis for the three LCZ buildings and the three localities, respectively. In these cases, we consistently observe significant energy exports during the summer, and the %PEB index often reaches 100 %, especially for low-rise

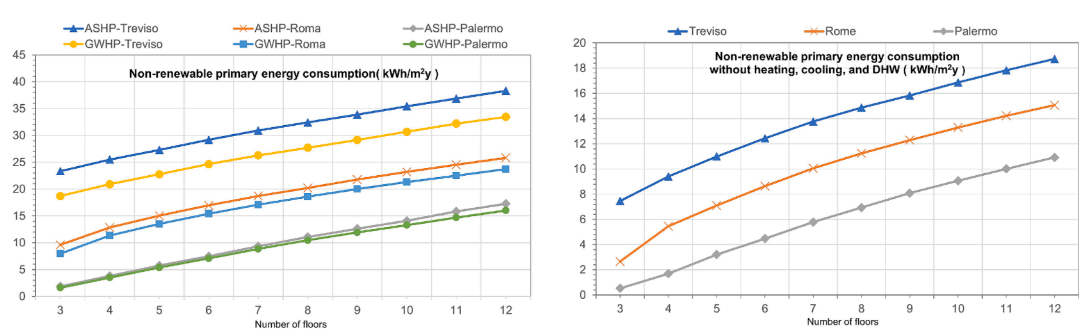

a) b)

Fig. 8. Specific annual non-renewable primary energy requirement (kWh/m^2·yr) of the analyzed buildings (a) and of the buildings without heating, cooling, and DHW demand (b).

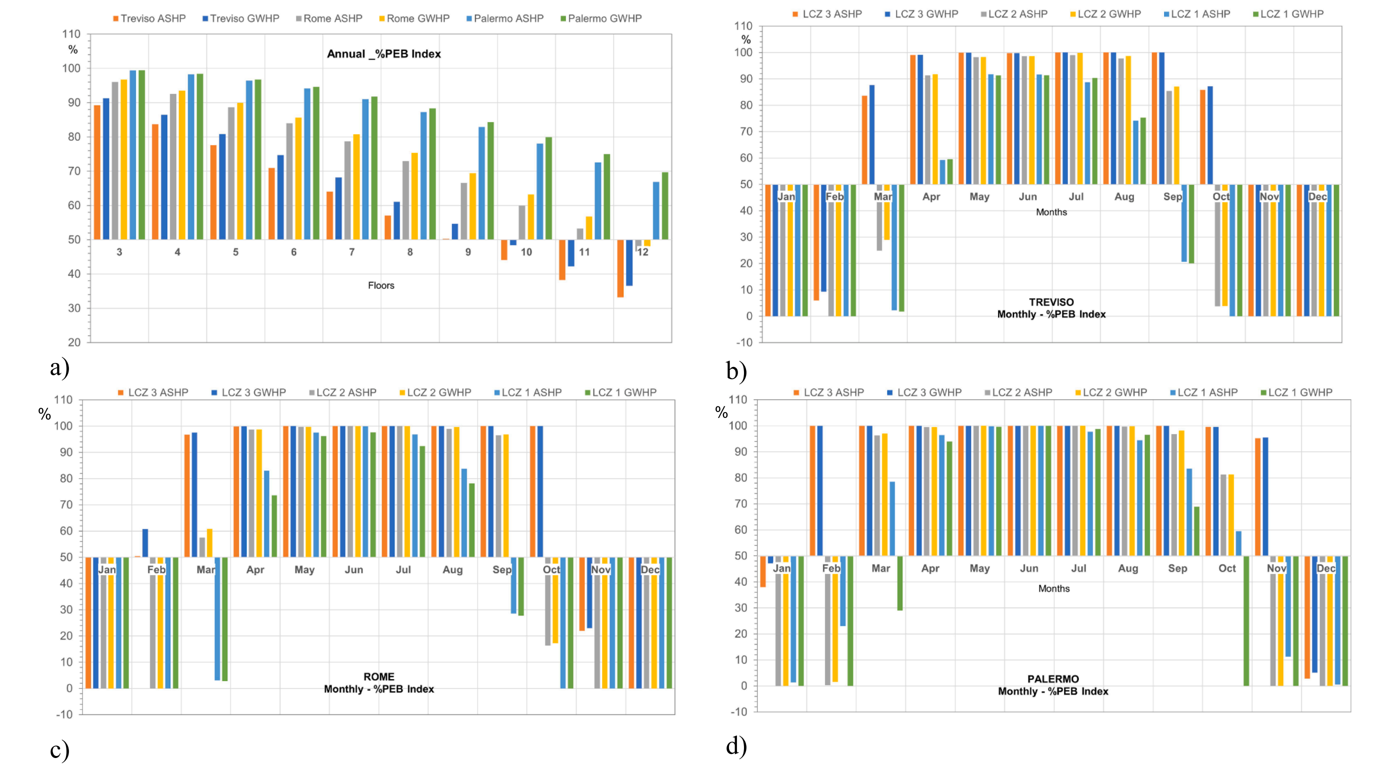

Fig. 9. Annual %PEB Indexes for ASHP and GWHP across all building sizes and localities (a), with the corresponding monthly %PEB Indexes reported for the three LCZs in each locality (b, c, d).

buildings. However, the situation is quite different in winter. In Treviso, the analyzed buildings are generally not PEBs, and their monthly %PEB is close to zero. The only exceptions are in March and October, when the two LCZ 3 buildings are PEBs. In Rome, the PEBs are the same as in Treviso, with the addition of the LCZ 3 buildings in February. Notably, in Palermo, none of the buildings are PEBs in December, and their %PEB index is close to zero. LCZ 1 and LCZ 2 buildings are not PEBs between November and February.

In conclusion, we observe that high %PEB values and the availability of PV energy for export are concentrated in the more favorable seasons and are limited during the winter months. Even buildings with significant annual %PEB values require non-renewable electric energy from the grid in amounts greater than their exported quota during the coldest months. In brief, these buildings can supply PV energy to the grid during months generally characterized by abundant national PV production, while remaining primarily consumers of grid electricity during months with lower PV production. It is clear that the behavior of a PEB must be analyzed at least on a monthly level. It is important to highlight that the share of renewable energy available on the grid is never sufficient to counterbalance the negative impact on the %PEB caused by inadequate local energy production. This underscores a critical weakness: the limited availability of renewable energy on the grid during such periods. Based on previous definitions of PEB, efforts are primarily focused on reducing building energy demand and increasing the amount of renewable energy produced locally. However, the introduction of a new PEB definition has also highlighted the importance of reducing the non-renewable share of energy imported from the grid. To meet the new PEB standard, reducing this non-renewable share is now a priority over reducing the total amount of imported energy.

A key forward-looking strategy must focus on strengthening renewable energy supply at the grid level. This entails expanding renewable systems specifically for the public grid, with a focus on established technologies like hydropower, wind, geothermal, large-scale photovoltaics, and biomass. A balanced mix of these sources is essential to maintain stable energy production, even when some are less effective due to seasonal or operational constraints.

Increased renewable production from energy communities, coordinated through the grid, is also crucial. Introducing large-capacity electrical storage will further support grid stability. Additionally, a pricing structure favoring renewable energy use and storage can accelerate the development of renewable energy grids.

4. Conclusion

Across various ASHRAE climate zones in southern Europe and for different urban forms already retrofitted according to national standards, the study investigated the effects of high-efficiency HPs and the extensive use of rooftop PV systems. The focus was on achieving either zero non-renewable energy consumption or meeting the PEB condition. The selection of GWHP over ASHP demonstrated potential energy savings of up to 8.4 % in comparison to ASHP electricity consumption. For these retrofitted urban forms, the energy contribution of rooftop PV systems was incorporated into hourly simulations. Firstly, the study highlighted the importance of optimizing electric storage system sizes for each case. The nominal power of the PV device alone is insufficient for determining battery capacity. For the same PV system, the correct capacity depends on the building's electric demand characteristics and actual PV production, which varies with climatic conditions, particularly solar radiation availability. The variability in both demand and production heavily influences battery performance. Therefore, annual dynamic simulations of the integrated building-PV system's performance are crucial for obtaining accurate results. At least on an hourly basis, the comparison between the electrical trends of demand and production can determine the PV quotas utilized by the building or exchanged with the battery or the public grid. This approach helps to identify the energy advantage of the battery for each storage capacity. Consequently, an economic cost-benefit analysis can be carried out. A simple payback analysis can provide a clear indication for selecting the most appropriate battery capacity.

The study concluded that rooftop PV systems alone cannot fully cover the electricity demand of the analyzed buildings. A portion of electricity must still be supplied by the public grid. Retrofit interventions to further improve the thermal performance of the building envelope can reduce heating and cooling loads, but even significant upgrades cannot entirely eliminate this reliance on the grid. Similarly, connecting buildings to a district heating network, classified as a renewable energy source (RES), can offset the thermal loads managed by electric HPs, yet some electricity will still need to be drawn from the grid. This finding emphasizes the importance of reducing electricity consumption from appliances and lighting, an aspect often overshadowed by efforts to enhance building performance rather than improve the efficiency of electric devices.

In conclusion, it is currently impossible for the LCZ types considered in this study to achieve zero non-renewable energy consumption from the grid on an annual basis. A more realistic goal is balancing the non-renewable and renewable electricity flows entering and leaving the building aligning with the new PEB definition. This analysis shows that, in many cases, achieving PEB status on an annual basis is feasible. However, even in these cases, monthly evaluations reveal the need for grid electricity during less sunny months. Therefore, achieving PEB status requires reducing the non-renewable quota delivered by the grid, which can be accomplished by increasing public grid generation from RES and integrating the studied buildings into renewable energy communities (RECs). Finally, while some methodological choices may appear limiting, they were adopted to ensure that the results were as accurate and context-specific as possible. The study accounted for the specific climatic, technological, and economic conditions, providing realistic findings and avoiding excessive generalizations. This rigorous approach offers a solid foundation for addressing the challenges explored and can be adapted for future studies across other geographic areas with different parameters.

CRediT authorship contribution statement

Luigi Schibuola: Writing – original draft, Supervision, Methodology, Data curation, Conceptualization. **Chiara Tambani:** Writing – original draft, Visualization, Validation, Software, Methodology, Investigation, Data curation, Conceptualization.

Declaration of competing interest

The authors declare that they have no known competing financial interests or personal relationships that could have appeared to influence the work reported in this paper.

Data availability

Data will be made available on request.

References

[1] [1] W.F. Lamb, T. Wiedmann, J. Pongratz, R. Andrew, M. Crippa, J.G.J. Olivier, D. Wiedenhofer, G. Mattioli, A. Al Khourdajie, J. House, S. Pachauri, M. Figueroa, Y. Saheb, R. Slade, K. Hubacek, L. Sun, S.K. Ribeiro, S. Khennas, S. de la Rue du Can, L. Chapungu, S.J. Davis, I. Bashmakov, H. Dai, S. Dhakal, X. Tan, Y. Geng, B. Gu, J. Minx, A review of trends and drivers of greenhouse gas emissions by sector from 1990 to 2018, Environmental Research Letters 16 (2021) 073005. https://doi.org/10.1088/1748-9326/abee4e.

[2] M. González-Torres, L. Pérez-Lombard, J.F. Coronel, I.R. Maestre, D. Yan, A review on buildings energy information: trends, end-uses, fuels and drivers, Energy Rep. 8 (2022) 626–637, https://doi.org/10.1016/J.EGYR.2021.11.280.

[3] European Commission, Roadmap to a Resource Efficient Europe, comunication, http://eur-lex.europa.eu/legal-content/EN/TXT/?uri=CELEX:52011DC0571 , 2011.

[4] P. Olasolo-Alonso, L.M. López-Ochoa, J. Las-Heras-Casas, L.M. López-González, Energy performance of buildings directive implementation in southern European countries: a review, Energy Build. 281 (2023) 112751, https://doi.org/10.1016/J.ENBUILD.2022.112751.

[5] C. Maduta, D. D'Agostino, S. Tsemekidi-Tzeiranaki, L. Castellazzi, G. Melica, P. Bertoldi, Towards climate neutrality within the European Union: assessment of the energy performance of buildings directive implementation in member states, Energy Build. 301 (2023) 113716, https://doi.org/10.1016/J.ENBUILD.2023.113716.

[6] European Union. Directive 2010/31/EU of the European Parliament and of the Council of 19 May 2010 on the energy performance of buildings (recast). 2010. Available from: https://eur-lex.europa.eu/LexUriServ/LexUriServ.do?uri=OJ:L:2010:153:0013:0035:EN:PDF., n.d.

[7] European Union, Energy Performance of Buildings Directive (EPBD), recast, 2024.

[8] European Union, 'Fit for 55' legislative package, commission work program, (2021).

[9] E. Özer, I. Imamovic, L. Kranzl, G. Azzolini, D.T. Silvia, F. Hugony, F. Zanghirella, National Building Renovation Plans and Zero-Emission Buildings, 2024.

[10] L.K. Wiginton, H.T. Nguyen, J.M. Pearce, Quantifying rooftop solar photovoltaic potential for regional renewable energy policy, Comput. Environ. Urban Syst. 34 (2010) 345–357, https://doi.org/10.1016/J.COMPENVURBSYS.2010.01.001.

[11] M. Ashraf Fauzi, N. Hanis Zainal Abidin, N. Mohd Suki, A. Mokhtar Albshir Budiea, Residential rooftop solar panel adoption behavior: Bibliometric analysis of the past and future trends, Renewable Energy Focus 45 (2023) 1–9. https://doi.org/10.1016/J.REF.2023.02.002.

[12] M. Alhuyi Nazari, J. Rungamornrat, L. Prokop, V. Blazek, S. Misak, M. Al-Bahrani, M.H. Ahmadi, An updated review on integration of solar photovoltaic modules and heat pumps towards decarbonization of buildings, Energy Sustain. Dev. 72 (2023) 230–242, https://doi.org/10.1016/J.ESD.2022.12.018.

[13] L. Schibuola, M. Scarpa, C. Tambani, Influence of charge control strategies on electricity import/export in battery-supported photovoltaic systems, Renew. Energy 113 (2017) 312–328, https://doi.org/10.1016/J.RENENE.2017.05.089.

[14] L. Schibuola, M. Scarpa, C. Tambani, Demand response management by means of heat pumps controlled via real time pricing, Energy Build 90 (2015) 15–28, https://doi.org/10.1016/J.ENBUILD.2014.12.047.

[15] N. Aste, C. Del Pero, F. Leonforte, S. Ounis, A.M.G. Abdelrahim, The role of photovoltaic technology in achieving net zero energy target in residential buildings, Energ. Strat. Rev. 55 (2024) 101543, https://doi.org/10.1016/J.ESR.2024.101543.

[16] C. Xiang, B.S. Matusiak, Facade integrated photovoltaic, state of the art of experimental methodology, IOP Conf. Ser. Earth Environ Sci. 352 (2019) 012062, https://doi.org/10.1088/1755-1315/352/1/012062.

[17] C. Marino, A. Nucara, M.F. Panzera, M. Pietrafesa, Towards the nearly zero and the plus energy building: primary energy balances and economic evaluations, Therm. Sci. Eng. Prog. 13 (2019) 100400.

[18] D. Kolokotsa, D. Rovas, E. Kosmatopoulos, K. Kalaitzakis, A roadmap towards intelligent net zero- and positive-energy buildings, Sol. Energy 85 (2011) 3067–3084.

[19] R.J. Cole, L. Fedoruk, Shifting from net-zero to net-positive energy buildings, Build. Res. Inf. 43 (2015) 111–120, https://doi.org/10.1080/09613218.2014.950452.

[20] A. Magrini, G. Lentini, S. Cuman, A. Bodrato, L. Marenco, From nearly zero energy buildings (NZEB) to positive energy buildings (PEB): the next challenge - The most recent European trends with some notes on the energy analysis of a forerunner PEB example, Dev. Built Environ. 3 (2020) 100019, https://doi.org/10.1016/J.DIBE.2020.100019.

[21] G.M.S. Kumar, S. Cao, State-of-the-art review of positive energy building and community systems, Energies (basel) 14 (2021), https://doi.org/10.3390/en14165046.

[22] M. Ala-Juusela, H. ur Rehman, M. Hukkalainen, F. Reda, Positive Energy Building Definition with the Framework, Elements and Challenges of the Concept, Energies (Basel) 14 (2021). https://doi.org/10.3390/en14196260.

[23] A.A.W. Hawila, R. Pernetti, C. Pozza, A. Belleri, Plus energy building: operational definition and assessment, Energy Build 265 (2022) 112069.

[24] M. Wronowski, Conceptual design of plus energy single family house in Warsaw, Poland, REHVA J. no. October (2013) 58–62., (n.d.).

[25] M. Bojić, N. Nikolić, D. Nikolić, J. Skerlić, I. Miletić, Toward a positive-net-energy residential building in Serbian conditions, Appl Energy 88 (2011) 2407–2419.

[26] "EXCESS | Resources." https://positive-energy-buildings.eu/resource? t=Report on the definition of a Positive Energy Building., (n.d.).

[27] S. Hamels, CO2 Intensities and Primary Energy Factors in the Future European Electricity System, Energies (basel) 14 (2021), https://doi.org/10.3390/en14082165.

[28] I. Sartori, A. Napolitano, K. Voss, Net zero energy buildings: a consistent definition framework, Energy Build 48 (2012) 220–232.

[29] A.J. Marszal, P. Heiselberg, J.S. Bourrelle, E. Musall, K. Voss, I. Sartori, A. Napolitano, Zero energy building – a review of definitions and calculation methodologies, Energy Build. 43 (2011) 971–979.

[30] M.J.N. Oliveira Panão, The overall renewable energy fraction: An alternative performance indicator for evaluating Net Zero Energy Buildings, Energy Build 127 (2016) 736–747. https://doi.org/https://doi.org/10.1016/j.enbuild.2016.06.057.

[31] G.A. Dávi, E. Caamaño-Martín, R. Rüther, J. Solano, Energy performance evaluation of a net plus-energy residential building with grid-connected photovoltaic system in Brazil, Energy Build. 120 (2016) 19–29.

[32] E. Rodriguez-Ubinas, C. Montero, M. Porteros, S. Vega, I. Navarro, M. Castillo-Cagigal, E. Matallanas, A. Gutiérrez, Passive design strategies and performance of Net Energy Plus Houses, Energy Build. 83 (2014) 10–22.

[33] J. Chai, P. Huang, Y. Sun, Investigations of climate change impacts on net-zero energy building lifecycle performance in typical Chinese climate regions, Energy 185 (2019) 176–189.

[34] H. Rehman, A. Hasan, F. Reda, Challenges in reaching positive energy building level in apartment buildings in the Nordic climate: a techno-economic analysis, Energy Build 262 (2022) 111991.
[35] A. Passer, C. Ouellet-Plamondon, P. Kenneally, V. John, G. Habert, The impact of future scenarios on building refurbishment strategies towards plus energy buildings, Energy Build. 124 (2016) 153–163.
[36] A. Bruck, S. Diaz Ruano, H. Auer, Values and implications of building envelope retrofitting for residential Positive Energy Districts, Energy Build. 275 (2022) 112493.
[37] X. Yang, M. Hu, A. Tukker, C. Zhang, T. Huo, B. Steubing, A bottom-up dynamic building stock model for residential energy transition: a case study for the Netherlands, Appl. Energy 306 (2022) 118060.
[38] W. Stutterecker, E. Blümel, Energy plus standard in buildings constructed by housing associations? Energy 48 (2012) 56–65.
[39] S. Thiers, B. Peuportier, Energy and environmental assessment of two high energy performance residential buildings, Build. Environ. 51 (2012) 276–284.
[40] Preferred Reporting Items for Systematic Reviews and Meta-Analyses: The PRISMA Statement, Ann Intern Med 151 (2009) 264–269. https://doi.org/10.7326/0003-4819-151-4-200908180-00135.
[41] V. Battaglia, L. Vanoli, C. Verde, P. Nithiarasu, J.R. Searle, Dynamic modelling of geothermal heat pump system coupled with positive-energy building, Energy 284 (2023) 128557.
[42] ASHRAE, Climatic Data for Building Design Standards., Https://Xp20.Ashrae.Org/Standard169/169_2013_a_20201012.Pd (2023).
[43] R. Gupta, J. Mathur, V. Garg, Assessment of climate classification methodologies used in building energy efficiency sector, Energy Build 298 (2023) 113549.
[44] I. Andresen, T. Healey Trulsrud, L. Finocchiaro, A. Nocente, M. Tamm, J. Ortiz, J. Salom, A. Magyari, L. Hoes-van Oeffelen, W. Borsboom, W. Kornaat, N. Gaitani, Design and performance predictions of plus energy neighbourhoods – case studies of demonstration projects in four different European climates, Energy Build 274 (2022) 112447.
[45] U.S. Department of Energy, EnergyPlus, Https://Energyplus.Net/. (2019).
[46] MISE 2020, national decree, Requisiti tecnici per l'accesso alle detrazioni fiscali per la riqualificazione energetica degli edifici, annex E, Ministry of Economic Development, 6 August 2020, n.d.
[47] DesignBuilder Software Ltd, DesignBuilder v 7.3 https://designbuilder.co.uk., (n.d.).
[48] I.D. Stewart, T.R. Oke, E.S. Krayenhoff, Evaluation of the 'local climate zone' scheme using temperature observations and model simulations, Int. J. Climatol. 34 (2014) 1062–1080.
[49] B. Bechtel, P.J. Alexander, J. Böhner, J. Ching, O. Conrad, J. Feddema, G. Mills, L. See, I. Stewart, Mapping Local Climate Zones for a Worldwide Database of the Form and Function of Cities, ISPRS Int J Geoinf 4 (2015) 199–219, https://doi.org/10.3390/ijgi4010199.
[50] M. Demuzere, J. Kittner, A. Martilli, G. Mills, C. Moede, I.D. Stewart, J. van Vliet, B. Bechtel, Global Map of Local Climate Zones (2022), https://doi.org/10.5281/zenodo.6364594.
[51] M. Demuzere, J. Kittner, A. Martilli, G. Mills, C. Moede, I.D. Stewart, J. van Vliet, B. Bechtel, A global map of local climate zones to support earth system modelling and urban-scale environmental science, Earth Syst. Sci. Data 14 (2022) 3835–3873, https://doi.org/10.5194/essd-14-3835-2022.
[52] A. Oliveira, A. Lopes, S. Niza, Local climate zones in five southern European cities: an improved GIS-based classification method based on Copernicus data, Urban Clim. 33 (2020) 100631, https://doi.org/10.1016/J.UCLIM.2020.100631.
[53] T. Iungman, S. Khomenko, E.P. Barboza, M. Cirach, K. Gonçalves, P. Petrone, T. Erbertseder, H. Taubenböck, T. Chakraborty, M. Nieuwenhuijsen, The impact of urban configuration types on urban heat islands, air pollution, CO2 emissions, and mortality in Europe: a data science approach, Lancet Planet Health 8 (2024) e489–e505, https://doi.org/10.1016/S2542-5196(24)00120-7.
[54] Mehits for Santa Caterina museum in Treviso https://uk.climaveneta.com/Web/News/2500.html., 2021.
[55] L. Schibuola, C. Tambani, Environmental impact and energy performance of groundwater heat pumps in urban retrofit, Energy Build 261 (2022) 111964, https://doi.org/10.1016/J.ENBUILD.2022.111964.
[56] En,, 14511-3:2019 Air conditioners, liquid chilling packages and heat pumps for space heating and cooling and process chillers, with electrically driven compressors Part 3: Tests, Methods n.d (2019).
[57] RHOSS. THAETY-THAESY 269÷296, technical bulletin K201325IT ed.4. 2019., n.d.
[58] RHOSS. TCHEY-THHEY 245÷2187, technical bulletin K20325EN ed.11. 2019., n.d.
[59] L. Schibuola, Heat pump seasonal performance evaluation: a proposal for a European standard, Appl. Therm. Eng. (2000), https://doi.org/10.1016/S1359-4311(99)00041-1.
[60] M. Dongellini, C. Naldi, G.L. Morini, Seasonal performance evaluation of electric air-to-water heat pump systems, Appl. Therm. Eng. (2015), https://doi.org/10.1016/j.applthermaleng.2015.03.026.
[61] S. In, K. Cho, B. Lim, C. Lee, Partial load performance test of residential heat pump system with low-GWP refrigerants, Appl. Therm. Eng. (2015), https://doi.org/10.1016/j.applthermaleng.2015.04.013.
[62] CEN, EN 14825:2018 Air conditioners, liquid chilling packages and heat pumps, with electrically driven, compressors, for space heating and cooling - Testing and rating at part load conditions and calculation of seasonal performance, 2018.
[63] M. Sandrine, Eurovent chiller certification key stones and futures challenges, REHVA J. (2013) 31–41.
[64] L. Schibuola, M. Scarpa, C. Tambani, Modelling Of Hvac System Components For Building Dynamic Simulation, in: 2013. https://doi.org/10.26868/25222708.2013.2303.
[65] Maxeon SunPower 3 400 W , Https://Sunpower.Maxeon.Com/Au/Sites/Default/Files/2019-07/Max3-400-390-370-Au_0.Pdf (n.d.).
[66] J.H. Eckstein, Detailed Modelling of Photovoltaic System Components (1990).
[67] J.A. Duffie, W.A. Beckman, Solar Engineering of Thermal Processes (2013).
[68] Ø. Ulleberg, HYDROGEMS Component Library for TRNSYS 15 User Manual, 2001.
[69] Tesla Powerwall, https://www.tesla.com/sites/default/files/pdfs/powerwall/Powerwall%202_AC_Datasheet_en_AU.pdf, n.d.
[70] Tesla Powerwall, Price list, https://www.tesla.com/it_IT/powerwall/get, (n.d.).
[71] HEPI Household Energy Price Index 2024, Https://Www.Energypriceindex.Com/Price-Data (n.d.).
[72] GSE, Servizio di ritiro dedicato, regole tecniche, https://www.gse.it/servizi-per-te/fotovoltaico/ritiro-dedicato, (2024).
[73] Articolo 13.4, "Allegato A", deliberazione AEEG 280/07, https://www.gse.it/documenti_site/Documenti%20GSE/Servizi%20per%20te/RITIRO%20DEDICATO/Altri%20contenuti/Prezzi%20medi%20RID%20aggiornato%208-2024.pdf#:~:text=Prezzi%20medi%20mensili%20per%20fascia%20oraria%20e%20zona%20di%20mercato, 2024.
[74] IEA International Energy Agency, Battery and Secure Energy Transitions, World Energy Outlook Special Report, April 2024., n.d.
[75] S. Cai, Y. Li, Incentive policy for battery energy storage systems based on economic evaluation considering flexibility and reliability benefits, Front Energy Res 9 (2021), https://doi.org/10.3389/fenrg.2021.634912.
[76] I. Gaspar, R. Castro, T. Sousa, Optimisation and economic feasibility of battery energy storage systems in electricity markets: the Iberian market case study, J Clean Prod 324 (2021) 129255.
[77] DM 26 giugno 2015, Applicazione delle metodologie di calcolo delle prestazioni energetiche e definizione delle prescrizioni e dei requisiti minimi degli edifici, 2015.
[78] TERNA S.p.A, https://dati.terna.it/download-center, (n.d.).